ISSN 1674-1056
http://cpb.iphy.ac.cn
http://iopscience.iop.org/cpb
中国物理 B
Chinese Physics
中国物理
Chinese Physics B

Effects of the Casimir force on the properties of a hybrid optomechanical system

Yi-Ping Wang(王一平), Zhu-Cheng Zhang(张筑城), Ya-Fei Yu(於亚飞), Zhi-Ming Zhang(张智明)

Citation: Chin. Phys. B . 2019, 28(1): 014202. **doi:** 10.1088/1674-1056/28/1/014202
Journal homepage: http://cpb.iphy.ac.cn; http://iopscience.iop.org/cpb

What follows is a list of articles you may be interested in

Generation of sustained optimal entropy squeezing of a two-level atom via non-Hermitian operation

Yan-Yi Wang(王彦懿), Mao-Fa Fang(方卯发)
Chin. Phys. B . 2018, 27(11): 114207. **doi:** 10.1088/1674-1056/27/11/114207

Multi-window transparency and fast-slow light switching in a quadratically coupled optomechanical system assisted with three-level atoms

Wan-Ying Wei(魏晚迎), Ya-Fei Yu(於亚飞), Zhi-Ming Zhang(张智明)
Chin. Phys. B . 2018, 27(3): 034204. **doi:** 10.1088/1674-1056/27/3/034204

Parallel generation of 31 tripartite entangled states based on optical frequency combs

Jing Zhang(张静), Yan-Fang Wang(王艳芳), Xiao-Yu Liu(刘晓宇), Rong-Guo Yang(杨荣国)
Chin. Phys. B . 2017, 26(12): 124205. **doi:** 10.1088/1674-1056/26/12/124205

Generation of squeezed vacuum on cesium D2 line down to kilohertz range

Jian-Feng Tian(田剑锋), Guan-Hua Zuo(左冠华), Yu-Chi Zhang(张玉驰), Gang Li(李刚), Peng-Fei Zhang(张鹏飞), Tian-Cai Zhang(张天才)
Chin. Phys. B . 2017, 26(12): 124206. **doi:** 10.1088/1674-1056/26/12/124206

Quantum feedback cooling of two trapped ions

Shuo Zhang(张硕), Wei Wu(吴伟), Chun-Wang Wu(吴春旺), Feng-Guang Li(李风光), Tan Li(李坦), Xiang Wang(汪翔), Wan-Su Bao(鲍皖苏)
Chin. Phys. B . 2017, 26(7): 074205. **doi:** 10.1088/1674-1056/26/7/074205

Effects of the Casimir force on the properties of a hybrid optomechanical system*

Yi-Ping Wang(王一平), Zhu-Cheng Zhang(张筑城), Ya-Fei Yu(於亚飞)†, and Zhi-Ming Zhang(张智明)‡

Guangdong Provincial Key Laboratory of Nanophotonic Functional Materials and Devices (School of Information and Optoelectronic Science and Engineering), Guangdong Provincial Key Laboratory of Quantum Engineering and Quantum Materials, South China Normal University, Guangzhou 510006, *China*

(Received 20 August 2018; revised manuscript received 7 October 2018; published online 21 December 2018)

We investigate the effects of the Casimir force on the output properties of a hybrid optomechanical system. In this system, a nanosphere is fixed on the movable-mirror side of the standard optomechanical system, and the nanosphere interacts with the movable-mirror via the Casimir force, which depends on the mirror–sphere separation. In the presence of the probe and control fields, we analyze the transmission coefficient and the group delay of the field-component with the frequency of the probe field. We also study the transmission intensity of the field-component with the frequency of a newly generated four-wave mixing (FWM) field. By manipulating the Casimir force, we find that a tunable slow light can be realized for the field-component with the frequency of the probe field, and the intensity spectrum of the FWM field can be enhanced and shifted effectively.

Keywords: quantum optics, optomechanics, quantum information and processing

PACS: 42.50.–p, 42.50.Wk, 42.50.Ex **DOI:** 10.1088/1674-1056/28/1/014202

1. Introduction

Cavity optomechanics[1,2] has been a rapidly developing research field since it was proposed. A prototypical cavity optomechanical system (OMS), generally composed of an optical cavity with one movable end mirror, couples the cavity field with a mechanical resonator through radiation pressure, which has witnessed rapid advances in recent years, leading to a variety of applications, such as optomechanically-induced transparency (OMIT),[3,4] quantum memory,[5,6] precision measurement of tiny objects,[7] storage of light,[8] single-photon routers,[9] phonon blockade,[10] and so on.

In the past decades, in view of the potential impact of fast light and slow light on modern photonic technology, researchers have a great interest in their realization. On the one hand, various techniques have been developed to realize fast light and slow light in atomic vapors and solid-state materials. For example, studies on slow light have made use of the technique of electromagnetically induced transparency (EIT) in atomic vapors or Bose–Einstein condensate (BEC).[11,12] Mirhosseini *et al.* have observed the dramatic enhancement in the fast light effect caused by electromagnetically induced absorption in warm rubidium vapor.[13] On the other hand, the fast and slow lights have also been observed in OMS,[14–18] which has paved the way toward real applications, such as telecommunication, interferometry, and signal processing.[19,20] Moreover, the four-wave mixing (FWM) response, as an exciting nonlinear optical phenomenon, has also aroused the widespread interest of researchers.[21–23]

In addition, many researchers have been exploring and harnessing the exotic quantum effect, for instance, the Casimir force,[24,25] which originates from the existence of vacuum zero-point energy.[26] In 1997, the Casimir force was first measured precisely by Lamoreaux,[27] followed by other experiments.[28–30] The measurements of the Casimir force for a very short distance are challenging in current experiments. However, with the great progress in fabricating and characterizing materials on the nanometer scale in recent years, it is possible to achieve the required strong Casimir force by altering optical properties or geometric structures of the interacting materials.[31–35] With the decrease of the size of on-chip devices, the Casimir force becomes increasingly important in micro- and nano-mechanical devices. Based on the Casimir force, many beautiful theories and experiments have been done, such as vacuum friction of motion,[36] non-touching bound of nano-particles,[37] nonlinear mechanical oscillations,[38] giant vacuum force near a transmission line,[39] Casimir effect between two micromachined silicon components,[40] and so on.

As the research of the OMS shows more and more important applications in the field of precision measurement, the effect of the Casimir force on the OMS is a problem to be considered. In this paper, we investigate the effects of the Casimir force on the optical response properties in a cavity optome-

*Project supported by the National Natural Science Foundation of China (Grant Nos. 11574092, 61775062, 61378012, 91121023, and 60978009), the National Basic Research Program of China (Grant No. 2013CB921804), and the Innovation Project of Graduate School of South China Normal University (Grant No. 2017LKXM090).

†Corresponding author. E-mail: yuyafei@m.scnu.edu.cn

‡Corresponding author. E-mail: zhangzhiming@m.scnu.edu.cn

© 2019 Chinese Physical Society and IOP Publishing Ltd

chanical system, where a nanosphere is fixed on one side of the movable mirror and coupled by the Casimir force, which depends on the mirror–sphere separation. As a comparison, our proposal here does not need any charged or magnetic object due to the fact that the Casimir force originates from the vacuum zero-point energy. It should be pointed out that by combining the OMS with the Casimir force, many interesting physical phenomena have been found. For example, Nie *et al.*[41] found that a steady-state optomechanical entanglement can be manipulated by the Casimir force. Besides, with a tunable Casimir force, Liu *et al.*[42] studied OMIT and found that a highly-controlled optical switch can be obtained. Motivated by these related studies, we notice that the OMS involving the Casimir force can strongly enhance nonlinearities and allow us to observe more abundant physical phenomena. In the presence of the probe and control fields, by manipulating the Casimir force, we find that a tunable slow light can be realized. Besides, we also find that the FWM intensity spectrum can be enhanced and shifted effectively.

This paper is organized as follows. In Section 2, we describe the model and solve the dynamical equations of the system. The transmission and the group delay of the probe field, and the output intensity of the FWM are displayed in Section 3. Finally, we summarize our main results in Section 4.

2. Model and Hamiltonian

As shown in Fig. 1, we consider a hybrid optomechanical system, where a gold-coated nanosphere is fixed on one side of the movable mirror. The cavity is driven simultaneously by a strong control field with frequency $\omega_{\rm L}$ and a weak probe field with frequency $\omega_{\rm p}$. Moreover, the nanosphere is coupled to the movable mirror via the Casimir force, which depends on the mirror–sphere separation. The Hamiltonian of the system can be written as

$$H_{\rm total} = \hbar\omega_{\rm c}a^{\dagger}a+\frac{p^2}{2m}+\frac{1}{2}m\omega_{\rm m}^2x^2-\hbar ga^{\dagger}ax-\frac{\pi^3\hbar cR}{720(d-x)^2} +{\rm i}\hbar(\varepsilon_{\rm L}a^{\dagger}{\rm e}^{-{\rm i}\omega_{\rm L}t}+\varepsilon_{\rm p}a^{\dagger}{\rm e}^{-{\rm i}\omega_{\rm p}t}-{\rm H.c.}), \quad (1)$$

where the first term is the free Hamiltonian of the single-mode cavity field with frequency $\omega_{\rm c}$ and annihilation (creation) operator a ($a^{\dagger}$). The second and third terms describe the free Hamiltonian of the movable mirror, where x and p represent the position and the momentum operator of the mechanical resonator with the eigenfrequency $\omega_{\rm m}$ and the effective mass m, respectively. The fourth term describes the interaction between the cavity field and the movable mirror with the optomechanical coupling $g=\omega_{\rm c}/L$, where L is the cavity length. The fifth term is the Hamiltonian describing the Casimir interaction between the movable mirror and the nearby gold-coated nanosphere. For a fixed sphere–mirror separation d, we use the result of the proximity force approximation $F_{\rm c}=2\pi^3\hbar cR/720d^3$ (for $d/R\ll 1$),[43] where c is the speed of light in the vacuum, and R is the radius of the sphere. The sixth term describes the interaction of the cavity field with the control field (the probe field), with the amplitude $\varepsilon_{\rm L}=\sqrt{2\kappa\wp_{\rm L}/\hbar\omega_{\rm L}}$ ($\varepsilon_{\rm p}=\sqrt{2\kappa\wp_{\rm p}/\hbar\omega_{\rm p}}$); here $\wp_{\rm L}$ ($\wp_{\rm p}$) is the power of the control (probe) field, and κ is the decay rate of the cavity field.

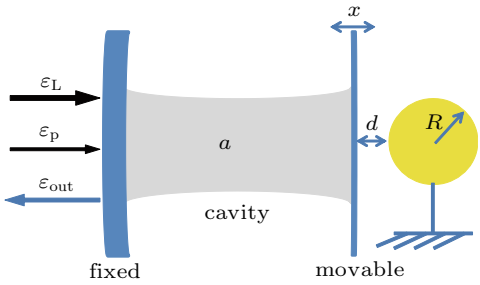


Fig. 1. Schematic diagram of the proposed hybrid optomechanical system. The Fabry–Pérot cavity contains a movable mirror, which interacts with both the cavity field via the radiation pressure and the nearby fixed gold-coated nanosphere via the Casimir force. In addition, the system is simultaneously driven by a strong control field with amplitude $\varepsilon_{\rm L}$ and a weak probe field with amplitude $\varepsilon_{\rm p}$. $\varepsilon_{\rm out}$ is the amplitude of the output field, and x describes the deviation of the mirror from its equilibrium position.

In the frame rotating with the frequency $\omega_{\rm L}$ of the control field, the Hamiltonian of the system can be rewritten as

$$H_{\rm total} = \hbar\Delta_{\rm c}a^{\dagger}a+\frac{p^2}{2m}+\frac{1}{2}m\omega_{\rm m}^2x^2-\hbar ga^{\dagger}ax-\frac{\pi^3\hbar cR}{720(d-x)^2} +{\rm i}\hbar(\varepsilon_{\rm L}a^{\dagger}+\varepsilon_{\rm p}a^{\dagger}{\rm e}^{-{\rm i}\delta t}-{\rm H.c.}), \quad (2)$$

where $\Delta_{\rm c}=\omega_{\rm c}-\omega_{\rm L}$ and $\delta=\omega_{\rm p}-\omega_{\rm L}$ are respectively the detunings of the cavity field frequency and the probe field frequency with respect to the control field frequency. The Heisenberg–Langevin equations can be written as

$$\dot{a}=-[\kappa+{\rm i}(\Delta_{\rm c}-gx)]a+\varepsilon_{\rm L}+\varepsilon_{\rm p}{\rm e}^{-{\rm i}\delta t}, \quad (3)$$

$$\ddot{x}+\gamma_{\rm m}\dot{x}+\omega_{\rm m}^2x+\frac{2V_{\rm s}}{m(d-x)^3}=\frac{\hbar g}{m}a^{\dagger}a, \quad (4)$$

where $V_{\rm s}=-\pi^3\hbar cR/720$, and $\gamma_{\rm m}$ is the decay rate of the movable mirror (here the noise terms are not included since we will only consider the mean value equations in the following part). Under the mean field approximation $\langle xa\rangle\approx\langle x\rangle\langle a\rangle$, and with $\langle 1/(d-x)^3\rangle\approx 1/(d-\langle x\rangle)^3$, the mean value equations are given by

$$\langle\dot{a}\rangle=-[\kappa+{\rm i}(\Delta_{\rm c}-g\langle x\rangle)]\langle a\rangle+\varepsilon_{\rm L}+\varepsilon_{\rm p}{\rm e}^{-{\rm i}\delta t}, \quad (5)$$

$$\langle\ddot{x}\rangle+\gamma_{\rm m}\langle\dot{x}\rangle+\omega_{\rm m}^2\langle x\rangle+\frac{2V_{\rm s}}{m(d-\langle x\rangle)^3}=\frac{\hbar g}{m}\langle a^{\dagger}\rangle\langle a\rangle, \quad (6)$$

which is a set of nonlinear equations. In order to obtain the solutions of these equations, we make the following ansatz:

$$\langle a\rangle=a_{\rm s}+a_{+}{\rm e}^{-{\rm i}\delta t}+a_{-}{\rm e}^{{\rm i}\delta t}, \quad (7)$$

$$\langle x\rangle=x_{\rm s}+x_{+}{\rm e}^{-{\rm i}\delta t}+x_{-}{\rm e}^{{\rm i}\delta t}. \quad (8)$$

The above equations contain three terms (O_s, O_+, and O_- ($O = a, x$)), where O_s is the steady-state solution of the system operator O in the absence of the probe field. For a weak probe field, $O_s \gg O_\pm$, hence equations (7) and (8) can be solved by treating $O_\pm$ as perturbations. After substituting Eqs. (7) and (8) into Eqs. (5) and (6), we obtain the following steady-state solutions:

$$a_s = \frac{\varepsilon_L}{\kappa + i(\Delta_c - g x_s)},$$
$$x_s = \frac{1}{m\omega_m^2}(\hbar g |a_s|^2 - \frac{2V_s}{(d-x_s)^3}), \tag{9}$$
$$a_+ = \frac{(\beta_- \alpha_+ m + i\hbar g^2 |a_s|^2)\varepsilon_p}{\beta_- \alpha_+ \alpha_- m - i\hbar g^2 |a_s|^2 (\alpha_+ - \alpha_-)}, \tag{10}$$
$$a_- = \frac{i\hbar g^2 |a_s|^2 \varepsilon_p}{\beta_+ \alpha_+^* \alpha_-^* m + i\hbar g^2 |a_s| (\alpha_+^* - \alpha_-^*)}, \tag{11}$$

where $\alpha_\pm = \kappa \mp i\Delta_c \pm i g x_s - i\delta$, and $\beta_\pm = \Omega_m^2 - \delta^2 \pm i\delta\gamma_m$ with $\Omega_m = \sqrt{\omega_m^2 + 6V_s/m(d-x_s)^4}$, which is the effective mechanical frequency.

In order to investigate the properties of the output filed, we use the input–output relation[44] $\varepsilon_{out}(t) = \varepsilon_{in}(t) - 2\kappa\langle a(t)\rangle$, and obtain

$$\begin{aligned}\varepsilon_{out}(t) &= (\varepsilon_L - 2\kappa a_s)e^{-i\omega_L t} + (\varepsilon_p - 2\kappa a_+)e^{-i\omega_p t} \\ &\quad - 2\kappa a_- e^{-i(2\omega_L - \omega_p)t} \\ &= \varepsilon_{outs} e^{-i\omega_L t} + \varepsilon_{out+} e^{-i\omega_p t} \\ &\quad + \varepsilon_{out-} e^{-i(2\omega_L - \omega_p)t},\end{aligned} \tag{12}$$

in which we have introduced

$$\begin{aligned}&\varepsilon_{outs} = \varepsilon_L - 2\kappa a_s, \quad \varepsilon_{out+} = \varepsilon_p - 2\kappa a_+, \\ &\varepsilon_{out-} = -2\kappa a_-,\end{aligned} \tag{13}$$

and they respectively correspond to the output fields with frequencies of the control field, of the probe field, and of a newly generated four wave mixing field.[21,45]

The transmission coefficient of the field with the frequency ω_p of the probe field can be written as

$$t_p(\omega_p) = \frac{\varepsilon_p - 2\kappa a_+}{\varepsilon_p} = 1 - \frac{2\kappa a_+}{\varepsilon_p}, \tag{14}$$

and its group delay can be defined as

$$\tau = \frac{d\phi_p}{d\omega_p}, \tag{15}$$

where $\phi_p = \arg[t_p(\omega_p)]$ is the phase of the output filed at the frequency ω_p. The group delay $\tau > 0$ and $\tau < 0$ correspond to the slow and fast light propagation,[46] respectively.

The output intensity of the FWM field (with frequency $(2\omega_L - \omega_p)$) can be defined as

$$I_{FWM} = \left|\frac{\varepsilon_{out-}}{\varepsilon_p}\right|^2 = \left|\frac{2\kappa a_-}{\varepsilon_p}\right|^2. \tag{16}$$

In the following sections, we numerically study the transmission (including the transmission coefficient and the group delay) of the field with the probe field frequency ω_p, and the output intensity of the FWM field with the frequency $(2\omega_L - \omega_p)$. The parameters used are analogous to those of Refs. [3], [21], [41], and [42], in which the cavity parameters are $\omega_c = 2\pi c/\lambda$, $\lambda = 1064$ nm, $L = 25$ mm, and $\kappa = 2\pi \times 80$ kHz. The parameters for the mirror and the nanosphere are $\gamma_m = 2\pi \times 141$ Hz, $\omega_m = 2\pi \times 947$ kHz, $m = 145$ ng, and $R = 150$ nm; the separation d is chosen as 1.5 nm$< d <$ 5 nm, as in Ref. [42]. Besides, we consider the red-detuned mechanical sideband, i.e., $\Delta_c = \omega_m$, and the system operates in the resolved sideband regime, i.e., $\kappa < \omega_m$. We should point out that, with the above parameters, we can obtain the ratio $x_s/d \lesssim 1.6 \times 10^{-2}$, which is consistent with that of Ref. [42].

3. Results and discussions

3.1. The transmission of the field-component with the probe field frequency ω_p

At first, we analyze the influence of the Casimir force on the transmission of the probe field. In Fig. 2(a), we plot the transmission spectra $|t_p(\omega_p)|^2$ of the probe field as a function of the detuning δ/ω_m for different mirror–sphere separations d. We also note that as the mirror–sphere separation d increases (in the range considered), the curves shift to the right (the larger detuning). From the figures, we observe that the transparency window displays an asymmetrical structure, which corresponds to the Fano resonances,[47,48] and is different from the symmetrical structure in the standard optomechanical system.

Figure 2(b) shows the change of the transmission $|t_p(\omega_p)|^2$ as a function of the mirror–sphere separation d at the resonant point $\delta = \omega_m$. It can be seen that the influence of the Casimir force on the transmission of the probe field is non-monotonic and non-linear, and there is a minimum for a certain d. We can adjust the transmission in the range $(0-1)$ by controlling d. As the authors of Ref. [42] have given a detailed discussion about the effect of the Casimir force on the transmission of the probe field, we will not discuss it again here.

Next, we explore the characteristics of the fast and slow light, described by the group delay of the transmitted probe field in our system. As shown in Fig. 3(a), the group delay τ of the transmitted probe field is plotted as a function of the detuning δ/ω_m for different mirror–sphere separations d. It can be seen that the group delay τ displays positive values, which corresponds to the slow light effects. Specifically, we observe that the group delay τ changes rapidly around the resonant point $\delta = \omega_m$. It can also be seen that with the increase

of d, the curves of the group delay shift to the right, and their peak intensity decreases.

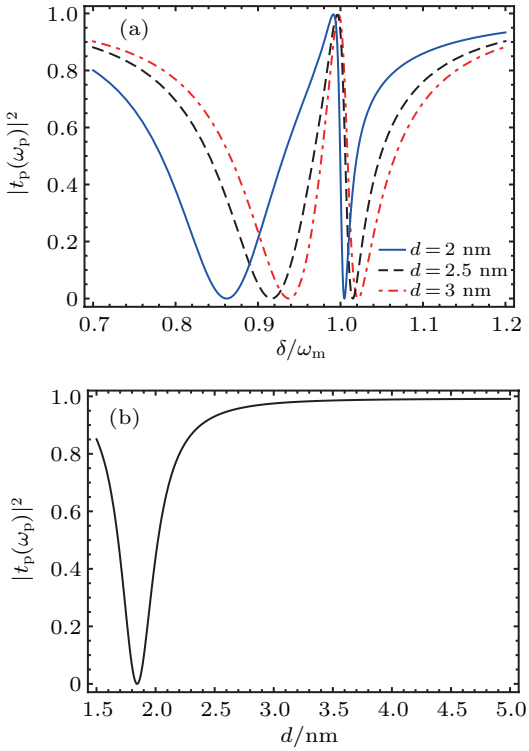


Fig. 2. (a) Plot of the transmission spectra $|t_p(\omega_p)|^2$ of the probe field as a function of the detuning δ/ω_m for the mirror–sphere separation $d = 2$ nm, 2.5 nm, and 3 nm. (b) Plot of the transmission spectrum $|t_p(\omega_p)|^2$ as a function of the mirror–sphere separation d for the case of $\delta = \omega_m$. Other parameters are $\wp_L = 1$ mW, $\lambda = 1064$ nm, $\kappa = 2\pi \times 80$ kHz, $L = 25$ nm, $\gamma = 2\pi \times 141$ Hz, $\omega_m = 2\pi \times 947$ kHz, $m = 145$ ng, and $R = 150$ nm.

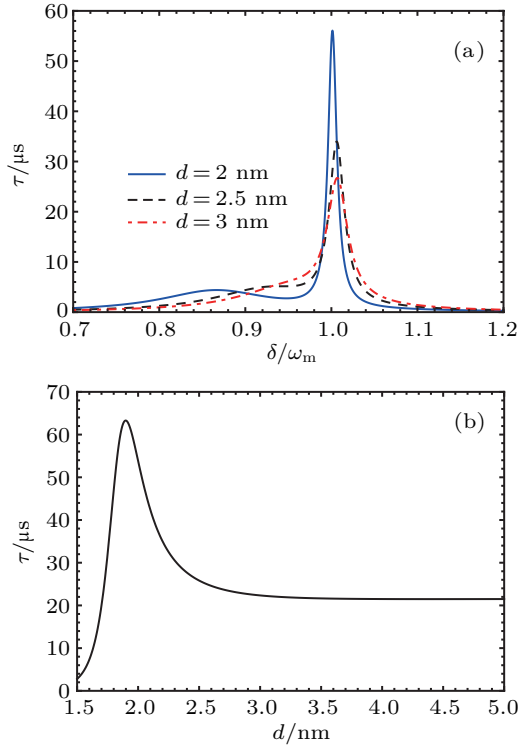


Fig. 3. (a) Plot of the group delay τ as a function of the detuning δ/ω_m for the mirror–sphere separation $d = 2$ nm, 2.5 nm, and 3 nm, and (b) plot of the group delay τ as a function of the mirror–sphere separation d for the case of $\delta = \omega_m$. Other parameters are the same as in Fig. 2.

Figure 3(b) shows the change of the group delay τ as a function of the mirror–sphere separation d at the resonant point $\delta = \omega_m$. It can be seen that the group delay τ displays positive values, which corresponds to the slow light effects. It can also be seen that the influence of the Casimir force on the group delay is non-monotonic and non-linear, and there is a maximum at about $d \approx 1.9$ nm, which corresponds to the slowest light. Therefore, we can adjust the speed of light by changing the mirror–sphere separation d.

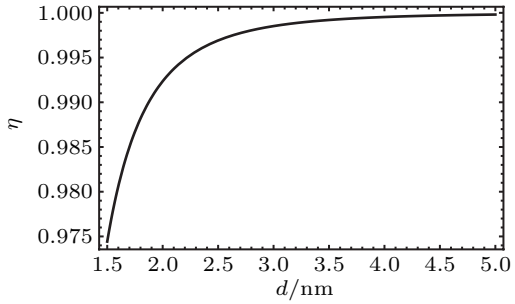


Fig. 4. Plot of of the ratio $\eta = \Omega_m/\omega_m$ as a function of the mirror–sphere separation d. Other parameters are the same as in Fig. 2.

Now we discuss the physical mechanism for these novel and interesting phenomena. The simultaneous presence of the control and probe fields can induce a radiation–pressure force oscillating at the frequency δ, which is close to the eigenfrequency ω_m of the movable mirror and causes the mirror to oscillate coherently. As a result, the Stokes field with the frequency $\omega_L - \omega_m$ and the anti-Stokes field with the frequency $\omega_L + \omega_m$ will emerge. Because our system is driven on the red sideband, the anti-Stokes field is resonantly enhanced and the Stokes field is suppressed. Moreover, the oscillation of the mirror will change the mirror–sphere separation, and therefore change the Casimir force and the effective mechanical frequency Ω_m. We confirm this behavior by plotting the ratio $\eta = \Omega_m/\omega_m$ as a function of the mirror–sphere separation d, as shown in Fig. 4. It can be seen that with the decrease of d (increase of the Casimir force), the effective mechanical frequency will decrease, that is, the mechanical resonant frequency is modified in the presence of the Casimir force. As a result, the anti-Stokes field will shift from the frequency $\omega_L + \omega_m$ to the frequency $\omega_L + \Omega_m$, which modifies the resonance condition and leads to the Fano resonances (Fig. 2(a)) and the shift of the group delay of the transmitted probe field (Fig. 3(a)).

From the above analysis, we can see that the transmission of the weak probe field is sensitive to the Casimir force. By changing the mirror–sphere separation, a tunable slow light effect can be achieved in our system, which can be used as an alternative method for controlling the light propagation.

3.2. The output intensity of the FWM field with the frequency $(2\omega_L - \omega_p)$

In this section, we study the effects of the Casimir force on the output intensity of the FWM field with the frequency $(2\omega_L - \omega_p)$. The FWM intensity spectrum I_{FWM} is plotted as a function of the detuning δ/ω_m in Fig. 5. From Fig. 5(a), we can see that there are two sharp and symmetrical peaks near $\delta \approx \pm\omega_m$, and the heights of the peaks increase with the decrease of d.

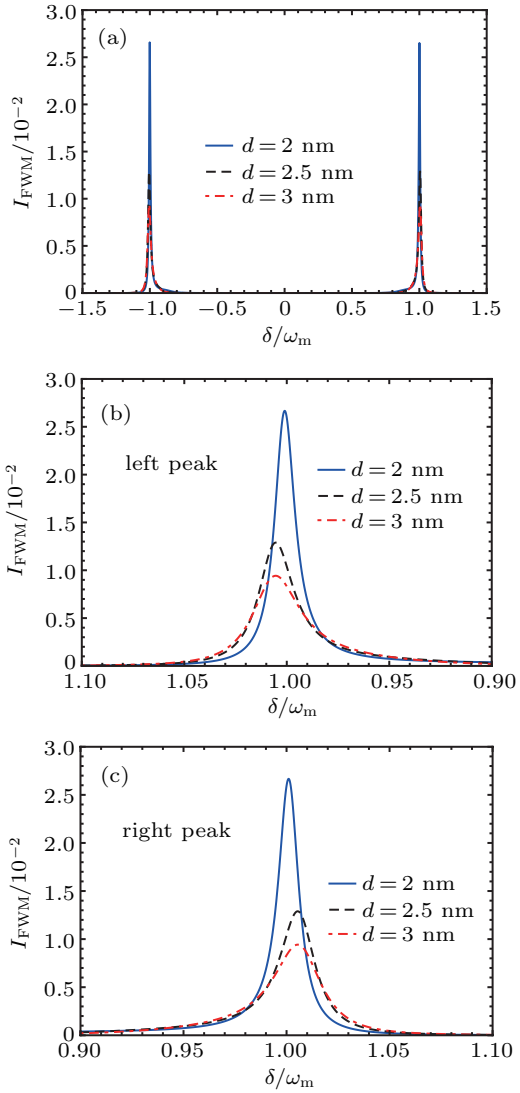


Fig. 5. Plots of the FWM intensity spectrum I_{FWM} as a function of the detuning δ/ω_m for the mirror–sphere separation $d = 2$ nm, 2.5 nm, and 3 nm. Other parameters are the same as in Fig. 2.

In order to observe the influence of the Casimir force on the FWM intensity more clearly, we enlarge the two peaks, as shown in Figs. 5(b) and 5(c). It can be seen that with the increase of d (in the range we considered), not only do the heights of the peaks decrease, but also the positions (in frequency) of the peaks shift toward outside.

We also plot the FWM intensity I_{FWM} as a function of the mirror–sphere separation d at the detuning $\delta = -\omega_m$, as shown in Fig. 6. It can be seen that the FWM intensity I_{FWM} is non-monotonic and non-linear as a function of d. There is a maximum at about $d \approx 1.9$ nm. The FWM intensity tends to a stable value with the increase of d. Similarly, this can also be understood through the fact that the presence of the Casimir force modifies the mechanical resonant frequency, i.e., $\omega_m \to \Omega_m$, as discussed in Fig. 4. Therefore, the intensity spectrum of the FWM field can be enhanced and shifted by the Casimir force.

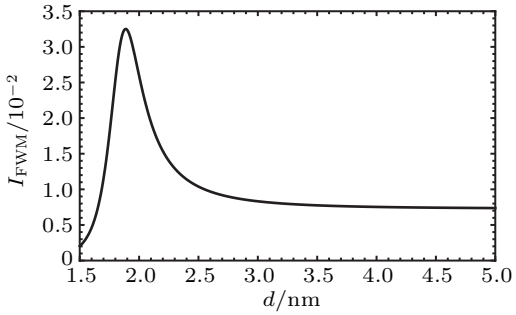


Fig. 6. Plot of the FWM intensity I_{FWM} as a function of the mirror–sphere separation d at the detuning $\delta = -\omega_m$. Other parameters are the same as in Fig. 2.

As clearly stated in Ref. [42], the Casimir force measurement for a small mirror–sphere separation is challenging in current experiments ($d = 1.5$–5 nm has been used in our calculations). However, by altering optical properties or geometric structures of the interacting materials,[31–35] it is still possible to significantly enhance the Casimir force even for a constant separation. For example, for parallel graphene layers, it was found that the Casimir force $F_c \sim d^{-5}$ with $d < 10$ nm, however, with specific nanostructures, the Casimir force F_c can be enhanced to d^{-7}.[35] That is, we can achieve the same level of Casimir force by using a larger separation in our proposal, which can meet the requirements of the experiment. In current experiments, the Casimir force has been accurately measured for $d \sim 100$ nm, which still shows an excellent agreement with theoretical predictions.[40,49] Thus, with efforts on controlling or enhancing the Casimir force, we expect that our results can be realized in experiments and have practical applications in the near future.

4. Conclusion

In conclusion, we have theoretically investigated the effects of the Casimir force on the output properties of a hybrid optomechanical system, including the transmission and the group delay of the field-component with the frequency ω_p of the probe field, and the output intensity of a new generated four-wave mixing field-component with the frequency of $(2\omega_L - \omega_p)$. We find that by manipulating the Casimir force, a tunable slow light transmission can be realized, and the intensity of the four-wave mixing field can be enhanced and shifted effectively.

References

[1] Braginskii V B and Manukin A B 1967 *Sov. Phys. JETP* **25** 653
[2] Liu Y L, Wang C, Zhang J and Liu Y X 2018 *Chin. Phys. B* **27** 024204
[3] Weis S, Riviere R, Deleglise S, Gavartin E, Arcizet O, Schliesser A and Kippenberg T J 2010 *Science* **330** 1520
[4] Wei W Y, Yu Y F and Zhang Z M 2018 *Chin. Phys. B* **27** 034204
[5] Qin L G, Wang Z Y, Wu S C, Gong S Q, Ma H Y and Jing J 2018 *Opt. Commun.* **410** 102
[6] Dong C, Wang H, Kuzyk M and Fiore V 2012 *Science* **338** 1609
[7] Zhang J Q, Li Y, Feng M and Xu Y 2012 *Phys. Rev. A* **86** 053806
[8] Chang D E, Naeini A H S, Hafezi M and Painter O 2011 *New J. Phys.* **13** 023003
[9] Agarwal G S and Huang S M 2012 *Phys. Rev. A* **85** 021801
[10] Shi H Q, Xie Z Q, Xu X W and Liu N H 2018 *Acta Phys. Sin.* **67** 044203 (in Chinese)
[11] Kasapi A, Jain M, Yin G Y and Harris S E 1995 *Phys. Rev. Lett.* **74** 2447
[12] Kien F L and Hakuta K 2009 *Phys. Rev. A* **79** 013818
[13] Mirhosseini M, Viza G I, Magaña-Loaiza O S, Malik M, Howell J C and Boyd R W 2016 *Phys. Rev. A* **93** 053836
[14] Jiang C, Liu H, Cui Y, Li X, Chen G and Chen B 2013 *Opt. Express* **21** 12165
[15] Teufel J D, Li D, Allman M S, Cicak K, Sirois A J, Whittaker J D and Simmonds R W 2011 *Nature* **471** 204
[16] Solanki S K, Lagg A, Woch J, Krupp N and Collados M 2003 *Nature* **425** 692
[17] Chen B, Jiang C and Zhu K D 2011 *Phys. Rev. A* **83** 055803
[18] Tarhan D, Huang S M and Müstecaplıoğlu Ö E 2013 *Phys. Rev. A* **87** 013824
[19] Chen H J, Chen C Z, Li Y, Fang X W and Tang X D 2017 *Opt. Commun.* **382** 73
[20] Boyd R W and Gauthier D J 2002 *Progress in Optics* (Wolf E Ed.) (Amsterdam: Elsevier) pp. 497–530
[21] Huang S M and Agarwal G S 2010 *Phys. Rev. A* **81** 033830
[22] Li J, Yu R, Ding C and Wu Y 2014 *Opt. Express* **22** 15024
[23] Li Z, You X, Li Y, Liu Y C and Peng K 2018 *Phys. Rev. A* **97** 033806
[24] Lamoreaux S K 2005 *Rep. Prog. Phys.* **68** 201
[25] Lamoreaux S K 2007 *Phys. Today* **60** 40
[26] Sushkov A O, Kim W J, Dalvit D A R and Lamoreaux S K 2011 *Nat. Phys.* **7** 230
[27] Lamoreaux S K 1997 *Phys. Rev. Lett.* **78** 5
[28] Ruoso G, Bressi G, Carugno G and Onofrio R 2002 *Phys. Rev. Lett.* **88** 041804
[29] Chan H B, Bao Y, Zou J, Cirelli R A, Klemens F, Mansfield W M and Pai C S 2008 *Phys. Rev.Lett.* **101** 030401
[30] Krause D E, Decca R S, Lopez D and Fischbach E 2007 *Phys. Rev. Lett.* **98** 050403
[31] Intravaia F, Koev S, Jung I W, Talin A A, Davids P S, Decca R S, Aksyuk V ADalvit D A and Lopez D 2013 *Nat. Commun.* **4** 2515
[32] Klimchitskaya G L, Mohideen U and Mostepanenko V M 2009 *Rev. Mod. Phys.* **81** 1827
[33] Rodriguez-Lopez P and Grushin A G 2014 *Phys. Rev. Lett.* **112** 056804
[34] Cysne T, Kort-Kamp W J M, Oliver D, Pinheiro F A, Rosa F S S and Farina C 2014 *Phys. Rev. A* **90** 052511
[35] Woods L M, Dalvit D A R, Tkatchenko A, Rodriguez-Lopez P, Rodriguez A W and Podgornik R 2016 *Rev. Mod. Phys.* **88** 045003
[36] Volokitin A I and Persson B N 2011 *Phys. Rev. Lett.* **106** 094502
[37] Rodriguez A W, McCauley A P, Woolf D, Capasso F, Joannopoulos J D and Johnson S G 2010 *Phys. Rev. Lett.* **104** 160402
[38] Chan H B, Aksyuk V A, Kleiman R N, Bishop D J and Capasso F 2001 *Phys. Rev. Lett.* **87** 211801
[39] Shahmoon E, Mazets I and Kurizki G 2014 *Proc. Natl. Acad. Sci. USA* **111** 10485
[40] Zou J, Marcet Z, Rodriguez A W, Reid M T H, McCauley A P, Kravchenko I I, Lu T, Bao Y, Johnson S G and Chan H B 2013 *Nat. Commun.* **4** 1845
[41] Nie W J, Lan Y H, Li Y and Zhu S Y 2012 *Phys. Rev. A* **86** 063809
[42] Liu X, Li Y and Jing H 2016 *Sci. Rep.* **6** 27102
[43] Bimonte G, Emig T, Jaffe R L and Kardar M 2012 *EPL* **97** 50001
[44] Gardiner C W and Zoller P 2000 *Quantum Noise: a Handbook of Markovian and non-Markovian Quantum Stochastic Methods with Applications to Quantum Optics* (Berlin: Springer–Verlag) vol. 56
[45] Boyd R W 2008 *Nonlinear Optics* (3rd edn.) (Amsterdam: Academic Press)
[46] Woodley J F and Mojahedi M 2004 *Phys. Rev. E* **70** 046603
[47] Fano U 1961 *Phys. Rev.* **124** 1866
[48] Cheng Y, Tan Z, Wang J, Zhu Y F and Zhan M S 2016 *Chin. Phys. Lett.* **33** 014202
[49] Garcia-Sanchez D, Fong K Y, Bhaskaran H, Lamoreaux S and Tang H X 2012 *Phys. Rev. Lett.* **109** 027202